

Dynamic status of lysosomal cathepsin in bovine oocytes and preimplantation embryos

Jianye LI¹⁾, Mana MAEJI¹⁾, Ahmed Zaky BALBOULA²⁾, Mansour ABOELENAIN³⁾, Takashi FUJII⁴⁾, Satoru MORIYASU⁴⁾, Hanako BAI¹⁾, Manabu KAWAHARA¹⁾ and Masashi TAKAHASHI^{5, 6)}

¹⁾Laboratory of Animal Genetics and Reproduction, Graduate School of Agriculture, Hokkaido University, Hokkaido 060-8589, Japan

²⁾Animal Sciences Research Center, College of Agriculture, Food & Natural Resources, University of Missouri, Columbia, MO 65211, USA

³⁾Department of Theriogenology, Faculty of Veterinary Medicine, Mansoura University, Mansoura 35516, Egypt

⁴⁾Animal Research Center, Hokkaido Research Organization, Hokkaido 081-0038, Japan

⁵⁾Graduate School of Global Food Resources(GSF), Hokkaido University, Hokkaido 060-0809, Japan

⁶⁾Global Station for Food, Land and Water Resources, Global Institution for Collaborative Research and Education(GI-CoRE), Hokkaido University, Hokkaido, 060-0815, Japan

Abstract. Lysosomal cathepsin, in particular cathepsin B (CTSB), plays an important role in implantation, pregnancy, and embryonic development. However, little is known about the mechanism related to the dynamic status of lysosomal cathepsins in bovine oocytes and preimplantation embryos. In the present study, we investigated the dynamics of gene expression, activity, and immunolocalization of CTSB, as well as the activities of lysosome, in bovine oocytes and preimplantation embryos. After gene expression analysis of several cathepsin-related genes, transcript levels of *CTSB*, *CTSD* and *CTSZ* were highest in Metaphase II (MII) oocytes followed by a significant decrease from the 8-cell embryo stage. Activity of CTSB showed a significant increase in 1-cell and morula stage embryos. Lysosomal activity was also significant higher in 1-cell and morula stages, which was consistent with CTSB activities. However, immunolocalization of CTSB did not show the similar pattern of CTSB and lysosomal activities. We also found significantly higher expression levels of *CTSB* transcript in the trophoctoderm (TE) compared to inner cell mass (ICM), whereas activity and immunolocalization of CTSB showed an opposite pattern, i.e. significantly higher in ICM than TE. These patterns were confirmed by the same analysis using separated ICM and TE. Our results suggest that lysosomal CTSB has a pivotal role during embryonic development and differentiation, especially fertilization and the differentiation period.

Key words: Cathepsin B, Cow, Lysosome, Oocytes, Preimplantation embryos

(J. Reprod. Dev. 66: 9–17, 2020)

Assisted reproductive technology, such as *in vitro* fertilization (IVF), offers great potential for improving the productivity of domestic animals. However, the overall efficiency of *in vitro* embryo production remains lower than that of *in vivo* production [1, 2]. Not all putative zygotes obtained from *in vitro* maturation (IVM) and IVF have the ability to develop into blastocysts. The capacity of development is determined by the quality of the oocytes and blastocysts produced by *in vitro* maturation and development, with high quality oocytes and blastocysts showing the capacity for successful development [3]. In general, oocyte and embryo quality is evaluated morphologically [4]. However, this evaluation does not correlate with embryo quality [5]. Thus, it is important to understand the mechanisms of development and differentiation prior to regulating

the quality of preimplantation embryos.

Cathepsins (CTSs) are ubiquitous proteases, which belong to the aspartic, cysteine, or serine protease families that catalyze the hydrolysis of proteins. CTSs regulate a variety of normal biological processes such as cell death, proliferation, migration, protein turnover, and cancer [6]. Different types of CTSs have different intracellular catabolic roles during differentiation and development. Knockdown of cathepsin D (CTSD) at oocyte fertilization during zebrafish development showed diseased muscle fibers [7]. Furthermore, expression of *CTSB* and D was upregulated during mouse trophoblast differentiation and this was necessary for normal embryo development and uterine decidualization [8, 9]; expression was also upregulated in the endometria of early pregnant ewes, and showed increased activity during maternal-conceptus pregnancy recognition [10, 11]. Protein expression levels of cathepsin B (CTSB) and D was high from the 1-cell to morula stage, and pharmacological inhibition of CTSB and D arrested embryonic development until the morula stage [12]. The cathepsin family, in particular CTSB, has important roles in implantation, pregnancy [9], and embryonic development. CTSB showed a remarkable sensitivity to the zona pellucida (ZP), acted in zona lysis, and was responsible for hatching of hamster blastocysts

Received: September 12, 2019

Accepted: October 15, 2019

Advanced Epub: November 3, 2019

©2020 by the Society for Reproduction and Development

Correspondence: M Takahashi (e-mail: mmasashi@anim.agr.hokudai.ac.jp)

This is an open-access article distributed under the terms of the Creative Commons Attribution Non-Commercial No Derivatives (by-nc-nd) License. (CC-BY-NC-ND 4.0: <https://creativecommons.org/licenses/by-nc-nd/4.0/>)

[13, 14]. Other roles of CTSB on cellular function and embryo quality have been elucidated. Recent studies have revealed higher CTSB expression and activity in poor quality bovine and porcine embryos, in which inhibition of CTSB activity increased the developmental competence of both bovine and porcine preimplantation embryos by decreasing apoptosis levels through preventing cytochrome c release [15, 16]. Giving the inverse relationship between apoptosis and embryo quality, it is plausible that higher CTSB activity was observed in poor quality and heat-shocked bovine oocytes when compared to controls [17, 18]. Inhibiting CTSB activity in oocytes and embryos increased the developmental rate and embryo quality [16, 17], indicating that lysosomal CTSB regulation in relation to lysosomal status is a promising strategy for improving the quality of *in vitro* produced (IVP) embryos.

Lysosomes are ubiquitous and specialized intracellular organelles that constitute 0.5 to 5.0% of the cell volume [19] and consist of the primary degradative compartments of the cell including protease cathepsins. The lysosomes receive degraded substrates through several pathways, including endocytosis, phagocytosis, and autophagy [12]. In recent years, it has been demonstrated that lysosomes participate in many physiological processes and not restricted to degradation. Therefore, mutation of genes involved in lysosomal function can lead to lysosomal dysfunction and disease, such as Danon disease and lysosomal storage disorders [20]. In particular, the distribution and functional analyses of lysosomes during mouse preimplantation embryo development revealed that the characteristics of lysosomes varied during preimplantation development [12]. Moreover, lysosomal dysfunction using genetic knockdown and pharmacological inhibition showed adverse effects on preimplantation embryos, and down-regulation of lysosome-associated membrane protein 1 and 2 (LAMP 1 and LAMP 2) in 1-cell mouse embryos resulted in embryonic arrest at the 2-cell stage [12]. Therefore, this developmental arrest indicates that lysosomal cathepsin machinery is important for mouse embryonic development.

These past findings highlight that lysosomal CTS-mediated machinery is a promising strategy for improving the quality of IVP embryos. However, the dynamic expression patterns of CTSs during oocyte maturation and preimplantation development remains poorly understood. Therefore, in this study, we investigated the catabolic enzymatic activity, protein localization of CTSB and mRNA transcript levels of *CTSB*, *CTSD*, and *CTSZ*, as well as lysosomal dynamic status during bovine oocyte maturation and development of preimplantation embryos.

Materials and Methods

Oocyte collection and IVM

Bovine ovaries were collected from a local abattoir and transported to the laboratory at 20°C. The ovaries were washed several times in sterile saline. Cumulus-oocyte complexes (COCs) were aspirated from follicles (2–8 mm in diameter) using a disposable 18-gauge needle attached to a 10-ml syringe, washed in PB1 medium, then matured and cultured in TCM-199 (Gibco, Grand Island, NY, USA) supplemented with 10 µM cysteamine (Sigma Aldrich, St. Louis, MO, USA), 10% (v/v) fetal bovine serum (FBS) (PAA Laboratories, QLD, Australia), 0.5 mg/ml follicle-stimulating hormone (Kyoritsu Seiyaku, Tokyo,

Japan), 100 U/ml penicillin (Nacalai Tesque, Kyoto, Japan), and 100 U/ml streptomycin (Nacalai Tesque) covered with liquid paraffin (Nacalai Tesque) for 22 h in a humidified atmosphere containing 5% CO₂. After collection, cumulus cells surrounding the germinal vesicle (GV) stage oocytes were removed by repeated pipetting and sampled for further experimentation. After *in vitro* maturation, cumulus cells of COCs were removed by repeated pipetting in the presence of 0.1% hyaluronidase for 2–3 min. Metaphase II (MII) oocytes that extruded the first polar body were used for further experiments.

IVF and in vitro culture

Frozen semen was thawed in warm water (38.5°C) for 30 sec. Spermatozoa were washed by centrifugation at 600 g for 7 min in Brackett and Oliphant (BO) medium containing 2.5 mM theophylline (Wako Pure Chemical Industries, Osaka, Japan) and 7.5 µg/ml heparin sodium salt (Nacalai Tesque). After removal of supernatant, the sperm pellet was diluted with IVF100 solution (Research Institute for the Functional Peptides, Yamagata, Japan) to make a final concentration of 5×10^6 /ml of spermatozoa pellet. The matured COCs were transferred to the prepared IVF100 sperm medium and cultured for 18 h at 38.5°C in a humidified atmosphere of 5% CO₂ and 5% O₂ in air.

After fertilization, presumptive zygotes were denuded by pipetting to remove cumulus cells and then cultured in Bovine KSOMaa medium (Zenith Biotech, Guilford, UK) containing 5% FBS, 100 U/ml penicillin and 100 U/ml streptomycin at 38.5°C in a humidified atmosphere of 5% CO₂ and 5% O₂ for 7 days. One-cell embryos were collected before starting IVC, while 8-cell stage embryos, morulae, and expanded blastocysts were sampled on days 2, 5, and 7, respectively. In addition, expanded blastocysts on day 7 were carefully separated using a micro-blade (Feather, Osaka, Japan) equipped with micromanipulator (Narishige, NY, USA) to obtain separated inner cell mass (ICM) with trophectoderm (TE) (ICM + TE) and TE alone (TE).

RNA extraction and quantitative real-time reverse transcription polymerase chain reaction (qRT-PCR)

Total RNA from three oocytes, embryos, separated ICM/TE and TE samples was isolated using a Super Prep™ Cell Lysis & RT Kit for qPCR (TOYOBO, Osaka, Japan) according to the manufacturer's instructions. The extracted RNA was immediately used for RT-PCR or stored at –80°C until analysis. After standardizing the RNA quantity using a NanoDrop spectrophotometer (Thermo Fisher Scientific, Wilmington, DE, USA), cDNA was then synthesized using the Super Prep™ Cell Lysis & RT Kit for qPCR (TOYOBO) including 5xRT Master Mix (2.7 µl) and Nuclease-free water (8 µl) containing 2.67 µl of RNA from the cell samples. Finally, qRT-PCR was performed to evaluate the expression of *CTSB*, *CTSD*, and *CTSZ* transcripts relative to histone *H2A* using Light Cycler® 480 (Roche, Basel, Switzerland). The primers used for the analysis are described in Table 1. The reactions were carried out in 96-well PCR plates, in a total volume of 10 µl containing 5 µl of Thunderbird SYBR qPCR Mix (TOYOBO), 1 µl of each primer (10 µM), and 3 µl of cDNA, and then subjected to the following cycling conditions: one cycle at 95°C for 30 sec, followed by 55 cycles at 95°C for 10 sec (denaturation), 55°C for 15 sec (primer annealing), and 72°C for 30 sec (extension). The relative expression levels of each of the target

Table 1. List of primers and primer sequences used for quantitative real-time reverse transcription polymerase chain reaction (qRT-PCR)

Genes	Primer Sequence (5'-3')	GenBank accession number
<i>CTSB</i>	F: CACTTGGAAGGCTGGACACA	NM_174031.2
	R: GCATCGAAGCTTTCAGGCAG	
<i>CTSD</i>	F: CCCGTGGAACACCTGATCGCCAA	NM_001166521.1
	R: CCCGATGCCGATCTCCCCGTA	
<i>CTSZ</i>	F: GGGAGAAGATGATGGCAGAAAT	NM_001077835.1
	R: TCTTTTCGGTTGCCATTATGC	
<i>H2A</i>	F: AGAGCCGGTTTGCAGTCCCG	NM_002106.4
	R: TACTCCAGGATGGCTGCGCTGT	

F: forward; R: reverse.

genes were calculated relative to that of histone *H2A*.

Detection of CTSB activity in oocytes and preimplantation embryos

Detection of CTSB activity in each stage of oocytes (GV, MII oocytes) and embryos (1-, 8-cell embryos, morulae, blastocysts) as well as separated ICM + TE and TE were carried out using Magic Red CTSB detection kit (MR-RR) (ImmunoChemistry Technologies, LLC, Bloomington, MN, USA), according to the manufacturer's instructions, at the indicated time points under constant fluorescence setting. In brief, at least five of each stage of oocytes and embryos were incubated in diluted Magic Red stock solutions dissolved in DMSO to 250 × with TCM-199 or KSOMaa at 38.5°C in a humidified atmosphere of 5% CO₂ for 45 min. To detect nuclei, Hoechst 33342 (Sigma-Aldrich) was supplemented with a concentration of 25 µg/ml in the reaction medium. After rinsing three times in phosphate buffered saline containing 0.2% polyvinyl alcohol (0.2% PVA-PBS), the freshly stained oocytes or embryos were mounted onto a glass-bottomed slide and immediately visualized under a BZ-9000 Bioevo fluorescence microscope (Keyence, Osaka, Japan) using a 550 nm excitation filter at 400 × magnification. In addition, to eliminate the fluorescence overlapping in ICM area with the blastocysts, CTSB activity of intact blastocysts was also observed under an inverted confocal laser scanning microscope with a 40 × immersion objective (Leica TCS SP5). All images of each stage or sample were obtained using the same exposure conditions and the intracellular fluorescence intensity of CTSB was analyzed by ImageJ software (National Institutes of Health, Bethesda, MD, USA).

Detection of lysosomal activity in oocytes and preimplantation embryos

To detect intracellular lysosomal localization, at least five of each stage of oocytes (GV, MII oocytes) and embryos (1- and 8-cell embryos, morulae, blastocysts) and separated ICM + TE and TE were incubated with 0.25 µl Lyso Tracker Red stock solution (L-7528, Molecular Probes, Eugene, OR, USA) in 250 µl TCM-199 or KSOMaa at 37°C in a humidified atmosphere of 5% CO₂ for 45 min. Nuclei staining was performed by adding 1 µl of Hoechst co-cultured with reaction medium. After incubation, samples were rinsed three times in 0.2% PVA-PBS. The freshly stained oocytes and embryos were mounted onto a glass-bottomed slide and immediately observed under

a fluorescence microscope (LAS X, Leica, Wetzlar, Germany) using a 550 nm excitation filter at 200 × magnification. All fluorescence images of each stage or sample were obtained using the same exposure conditions and analyzed by ImageJ software.

Immunohistochemical detection of CTSB in oocytes and preimplantation embryos

After removing the ZP using 0.1% (w/v) proteinase K (Sigma-Aldrich) in PB1 medium, at least five of each stage of oocytes (GV, MII oocytes) and embryos (1- and 8-cell embryos, morulae, blastocysts) were fixed by 4% paraformaldehyde (Wako Pure Chemical Industries) dissolved in PBS for 1 h at room temperature. After washing three times for 5 min each in 0.2% PVA-PBS, the oocytes and embryos were permeabilized using PVA-PBS containing 0.2% Triton X-100 for 1 h at room temperature. Then, samples were washed five times for 5 min each in washing solution containing 0.1% Triton X-100 and 0.3% BSA in PBS, and oocytes and embryos were incubated with a blocking solution of PBS containing 0.1% Triton X-100, 1% skim milk, and 5% FBS for 1 h at room temperature. Samples were then incubated overnight at 4°C with a primary antibody (Anti-cathepsin B Rabbit Polyclonal Antibody, EMD Millipore, Billerica, MA, USA) diluted to 1:500 in blocking solution. The samples incubated without the primary antibody as the negative control. After washing three times for 15 min each in washing solution, the samples were incubated in secondary antibody (Alexa Fluor 488-conjugated anti-rabbit IgG; Molecular Probes, Eugene, OR, USA) diluted to 1:200 in blocking solution and incubated for 1 h at room temperature. Finally, all samples were washed in washing solution five times at 5 min each and mounted onto a glass slide using VECTASHIELD with DAPI (Vector Laboratories, Burlingame, CA, USA) and observed under an inverted confocal laser scanning microscope with a 40 × immersion objective (Leica TCS SP5). The obtained images were analyzed using ImageJ software.

Statistical analysis

Data are representative of at least three independent experiments. All data are shown as the mean ± standard error of the mean (SEM). Statistically significant differences were assessed by student's *t*-test and one-way analysis of variance (ANOVA)-Tukey's Multiple Range Test implemented in Graphpad Prism[®] 7 Software (La Jolla, CA, USA). The relative comparison during different stages were

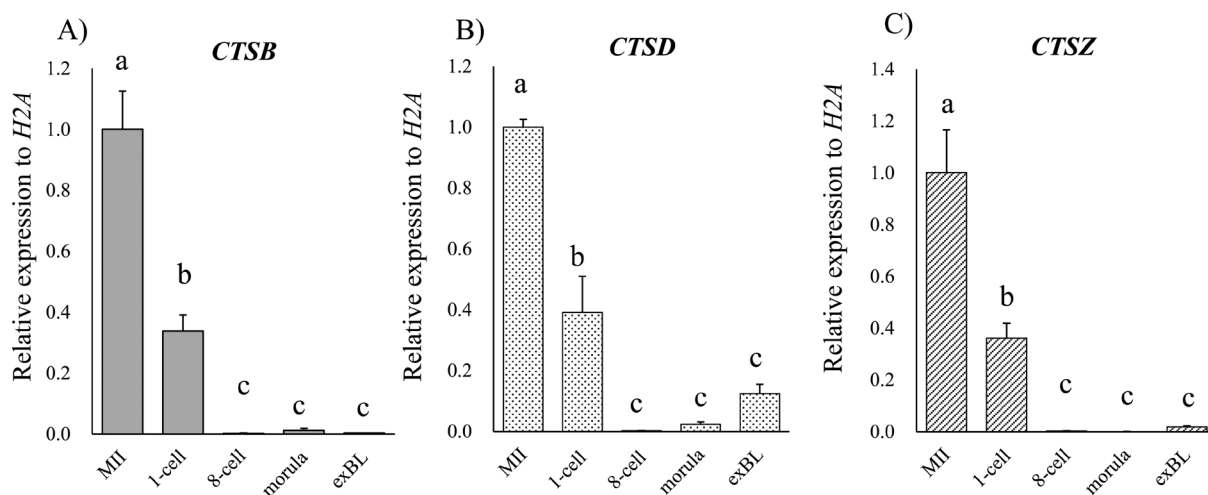


Fig. 1. Relative expression levels of cathepsin genes during various developmental stages measured by quantitative real-time reverse transcription polymerase chain reaction (qRT-PCR). The graphs show relative mRNA levels of *CTSB* (A), *CTSD* (B), and *CTSZ* (C) standardized by *H2A*. The expression level of each gene in the Metaphase II (MII) oocyte was set to one. Experiments were replicated five times. All data are shown as mean \pm SEM. Bars with different letters indicate statistical differences ($P < 0.01$).

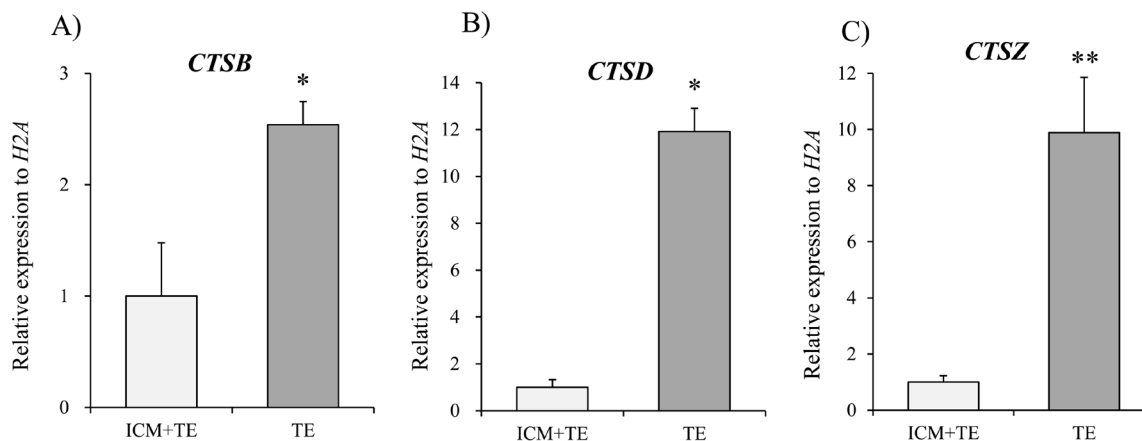


Fig. 2. Relative expression levels of cathepsin genes of separated inner cell mass (ICM) + trophectoderm (TE) and TE alone measured by quantitative real-time reverse transcription polymerase chain reaction (qRT-PCR). The graphs show relative mRNA levels of *CTSB* (A), *CTSD* (B), and *CTSZ* (C) standardized by *H2A*. The gene expression level of ICM + TE was set to one. Experiments were replicated five times. All data are shown as mean \pm SEM. Statistically significant differences are indicated by asterisks (* $P < 0.05$, ** $P < 0.01$).

used ANOVA, and student's *t*-test was used to compare the relative difference between ICM + TE and TE. P values < 0.001 , < 0.01 , or < 0.05 were considered statistically significant. P values < 0.1 were regarded as indicating a tendency.

Results

Expression levels of *CTSB*, *CTSD*, and *CTSZ* in oocytes and preimplantation embryos

The relative abundance of *CTSB*, *CTSD*, and *CTSZ* expression levels in bovine oocytes and each stage of preimplantation embryos were measured using qRT-PCR. To normalize the qRT-PCR reaction

efficiency, histone *H2A* was used as an internal standard. The levels of *CTSB*, *CTSD* and *CTSZ* transcripts were highest in the MII stage followed by a significant decrease from the 1-cell stage (Fig. 1A–C). Importantly, within the blastocyst, the *CTSB*, *CTSD* and *CTSZ* transcripts showed significantly higher expression in separated TE alone compared to separated ICM + TE (Fig. 2A–C). These results suggest that expression of CTs including *CTSB* plays some kind of role in differentiation of the ICM and TE.

CTSB activity in bovine oocytes and preimplantation embryos

Although gene expression levels of three CTs showed the developmentally specific pattern especially in ICM and TE in blastocyst,

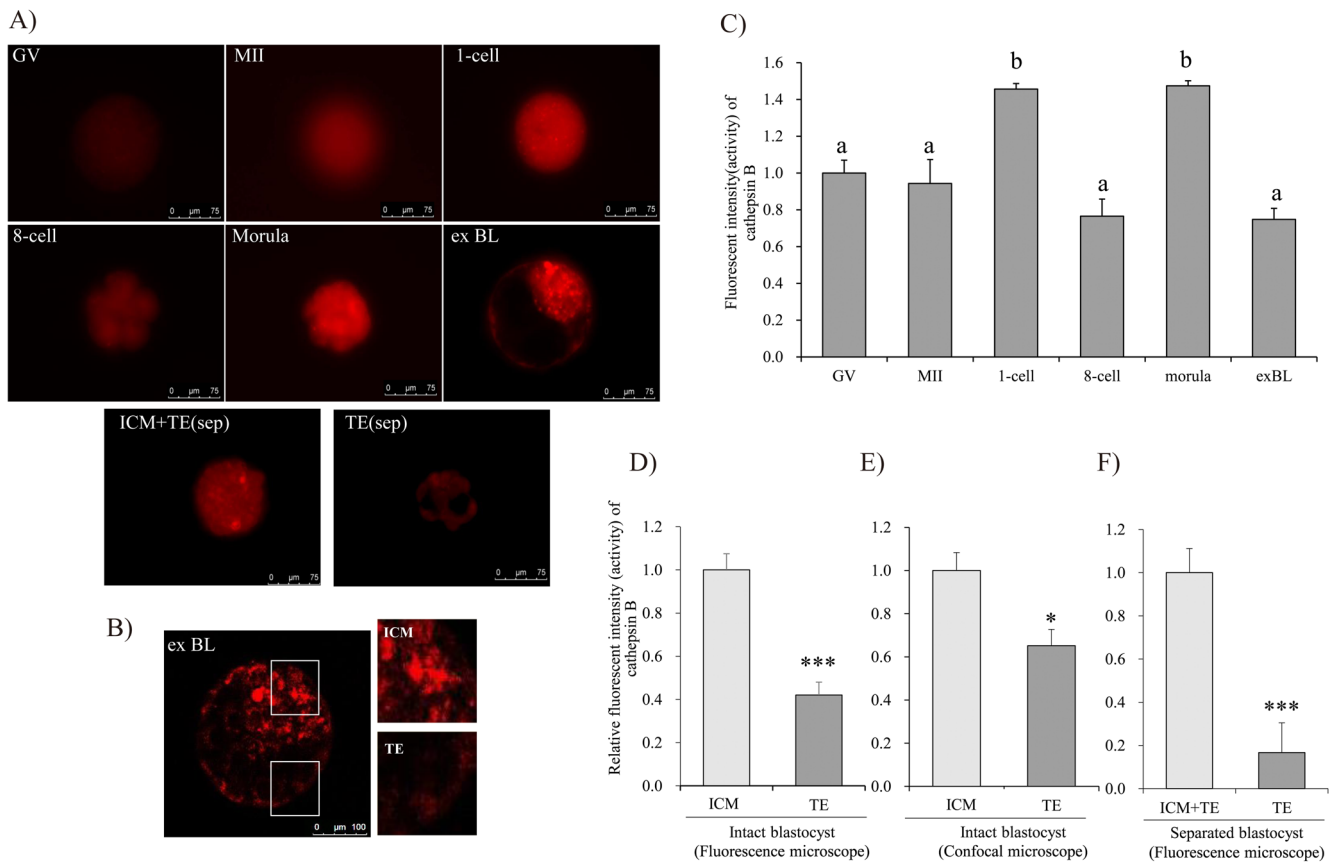


Fig. 3. Cathepsin B (CTSB) activity in each oocyte [germinal vesicle (GV), Metaphase II (MII) oocytes] and embryo (1-cell stage to expanded blastocysts, ex BL) stage. Photos show the fluorescent images of CTSB activity at different oocyte and embryo stages obtained by fluorescence microscope (A) and expanded blastocysts obtained by confocal microscope (B). Relative fluorescence intensity of CTSB (representing activity) at different oocyte and embryo stages (C), inner cell mass (ICM) and trophectoderm (TE) within the intact blastocysts (D, fluorescence microscope; E, confocal microscope), and separated ICM + TE and TE (F, fluorescence microscope). The scale bar represents 75 μ m and 100 μ m of the images obtained by fluorescence microscope and confocal microscope, respectively. Experiment was repeated three times. All data are shown as mean \pm SEM. Different letters indicate statistical difference ($P < 0.001$) between different stages. Asterisks indicate statistical difference (* $P < 0.05$, *** $P < 0.001$) between ICM + TE and TE.

we focused on CTSB dynamic expression patterns in the subsequent experiments because of availability of both antibody and fluorescent substrates for CTSB. To determine the dynamic status of CTSB activity on bovine oocytes and preimplantation embryos, GV, MII oocytes, 1-cell, 8-cell, morula embryos, and blastocysts, as well as separated ICM + TE and separated TE, were stained with Magic Red CTSB detection kit. CTSB activity was clearly observed to be localized in the cytoplasm, whereby activity was detected in the cytosol at each stage. Fluorescence representing CTSB activity was observed in each stage of oocytes and embryos (Fig. 3A). From image analysis, the intensity of CTSB fluorescence was significantly stronger in 1-cell and morula stages (Fig. 3C). On the other hand, the strong fluorescence of CTSB activity was detected in the ICM area of intact blastocysts both by fluorescence (Fig. 3A) and confocal microscope (Fig. 3B), as well as separated ICM + TE by fluorescence microscope (Fig. 3A) of the blastocyst. In the blastocyst stage embryo, strong fluorescence was detected in ICM compared to TE. Confocal imaging also showed the same difference in the fluorescent intensity between ICM and TE

as observed in epifluorescence microscopic detection. After image analysis, fluorescence intensity of CTSB was significantly higher in ICM within the intact blastocysts detected by fluorescence microscope (Fig. 3D) and confocal microscope (Fig. 3E), respectively. In addition, significantly higher fluorescence intensity was detected in separated ICM + TE than separated TE by fluorescence microscope (Fig. 3F).

Lysosomal activity in bovine oocytes and preimplantation embryos

To investigate the dynamic status of lysosomal activity in bovine oocytes and preimplantation embryos, we stained them with Lyso Tracker Red, which detects lysosomes with high specificity. Consistent with CTSB activity, we observed that lysosomal activity (fluorescence) was localized in the cytoplasm of each sample. The fluorescence intensity that is representative of lysosomal activity was higher in 1-cell and morula stage embryos with stronger fluorescence intensity (Fig. 4A). Furthermore, fluorescence intensity (i.e. lysosomal activity) was significantly stronger in 1-cell and morula stage embryos than

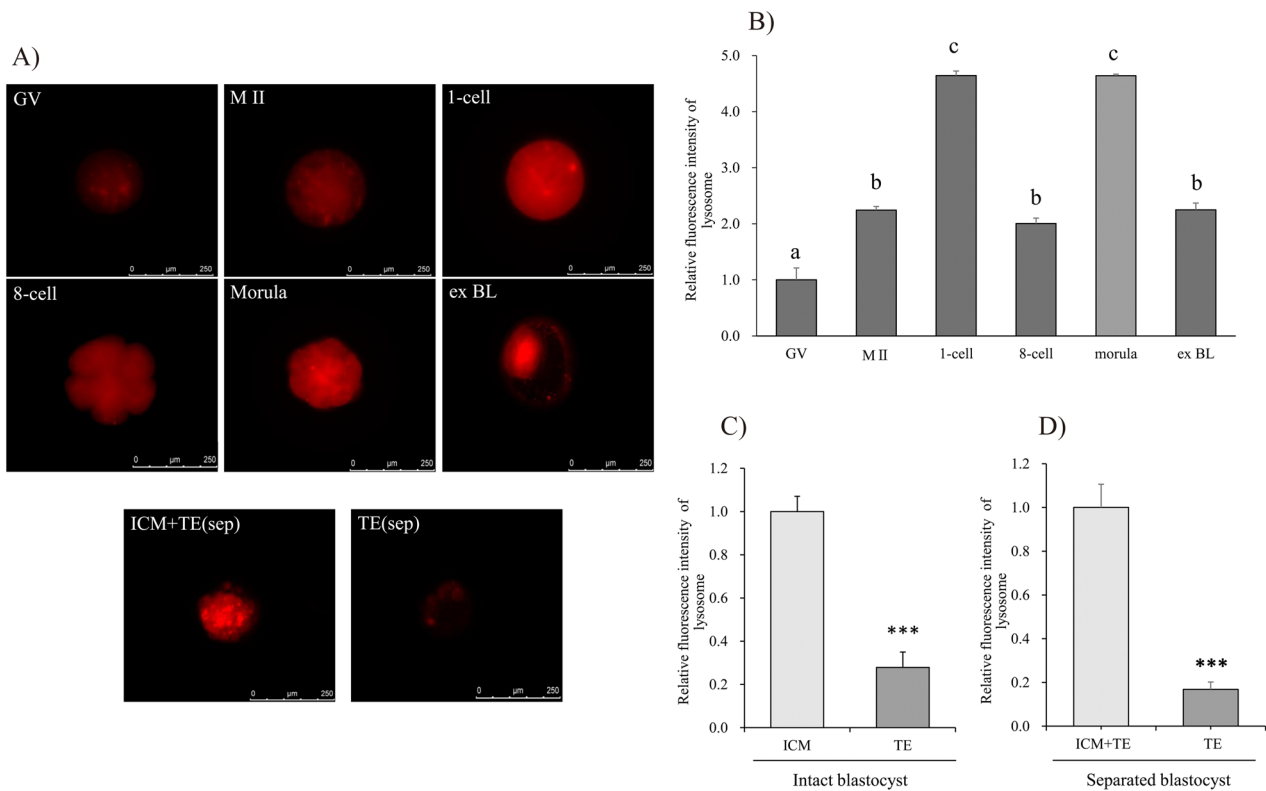


Fig. 4. Lysosomal activity in each oocyte [germinal vesicle (GV), Metaphase II (MII) oocytes] and embryo (1-cell stage to expanded blastocysts, ex BL) stage. Photos show the fluorescence images representing lysosomal activity at different oocyte and embryo stages (A). Relative fluorescence intensity (lysosomal activity) at different oocyte and embryo stages (B), separated inner cell mass (ICM) + trophectoderm (TE) and TE (C), and ICM + TE and TE within the whole blastocyst (D). The scale bar represents 250 μ m. Experiment was repeated three times. All data are shown as mean \pm SEM. Different letters indicate statistical difference (a, b vs. c: $P < 0.001$, a vs. b: $P < 0.05$) (B). Asterisks indicate statistical difference (***) $P < 0.001$) between ICM + TE and TE (C, D).

all other stages, and higher after the MII oocyte and subsequent embryo stages compared to GV oocyte stage (Fig. 4B). In addition, lysosomal activity was intact in both the ICM area and TE area (Fig. 4C) as well as dissected blastocyst (Fig. 4D).

Immunolocalization of CTSB in bovine oocytes and preimplantation embryos

To investigate whether the dynamic changes in CTSB activity at various stages of bovine oocytes and preimplantation embryos were accompanied by a difference in the amount and localization of CTSB proteins, immunostaining was performed in each stage. CTSB displayed a generally weak and uniform distribution in the cytoplasm of GV and MII oocytes, but stronger fluorescence was detected in the cytoplasm of the morula and blastocyst (Supplementary Fig. 1A: online only). Also, the fluorescence intensity was significantly higher in the morula and blastocyst stages compared to GV and MII oocytes (Supplementary Fig. 1B). Moreover, CTSB protein had significantly stronger fluorescence in the ICM area compared to that of the TE area within the blastocyst (Fig. 5A, B).

Discussion

Our results showed that mRNA transcription abundance of *CTSB*, *CTSD*, and *CTSZ* was high at the MII oocyte stage and expression significantly decreased by the 8-cell stage. Moreover, following the 8-cell stage, the expression of *CTSB*, *CTSD*, and *CTSZ* increased in the morula and blastocyst stages. The expression level of *CTSB*, *CTSD*, and *CTSZ* was significantly higher in the TE than ICM + TE. Consistent with the qRT-PCR profile of *CTSB*, CTSB activity supported by lysosomal distribution showed the highest activity just after fertilization and at the morula stage. These findings were supported by CTSB protein distribution which was clearly localized in the cytoplasm and significantly increased in the morula and blastocyst stage. Interestingly, in contrast to our qRT-PCR results, CTSB activity and protein expression within the blastocyst (both intact and separated) were significantly higher in the ICM than TE.

From the oocyte and zygote to early cleavage embryo, maternal proteins and RNAs are rapidly degraded and replaced by zygotic mRNAs and proteins. Early embryogenesis may rely on maternal protein stores as nutrients. Several maternal proteins are degraded by the ubiquitin-proteasome system like the lysosomal CTS family. However, the roles of lysosomal CTSs in oocyte maturation and

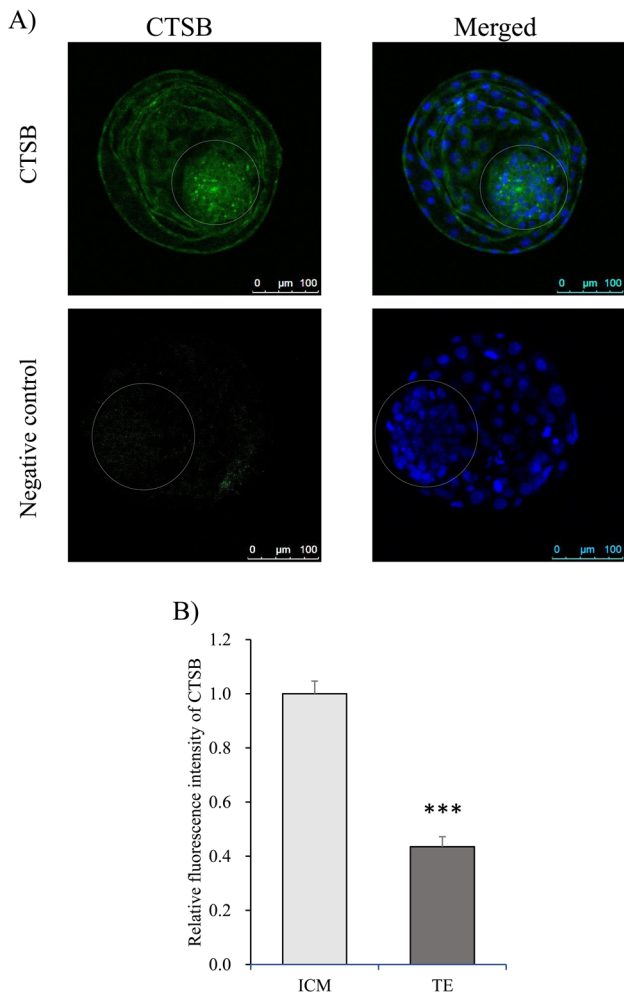


Fig. 5. Immunohistochemical detection of Cathepsin B (CTSB) in an expanded blastocyst. Photos show representative laser-scanning confocal microscopic images of CTSB and negative control in an expanded blastocyst (A). Blastocysts were stained with FITC-conjugated secondary antibody for anti-CTSB (green) and Hoechst 33342 for nuclei (blue). The white dot circle line circled the ICM area within the blastocyst. The merged images are presented in green (FITC) and blue (Hoechst 33342). Relative fluorescence levels of CTSB in the inner cell mass (ICM) and trophectoderm (TE) within the blastocyst (B). Experiment was repeated four times. All data are shown as mean \pm SEM. Asterisks indicate statistical difference (***) $P < 0.001$ between ICM and TE.

preimplantation embryo development remain poorly understood.

In mammals, protein degradation is accelerated shortly after fertilization and early embryogenesis relies on maternal protein stores as nutrients. Fertilization and early cleavage stages are initiated by maternal RNA and proteins accumulated during oogenesis and the final stages of oocyte maturation. In the post-fertilization shift from oocyte to embryo, maternal proteins in oocytes are degraded and new proteins encoded in the zygotic genome are synthesized. Large scale synthesis of mRNA from the diploid embryonic genome is initiated at a species-specific time point. The onset of embryonic genome

activation is considered to occur at the 8-cell stage in bovines [21]. A recent study demonstrated that autophagy influences maternal mRNA degradation in developing porcine parthenotes, which revealed that mRNA expression levels of *Atg5*, *Beclin 1*, and *LC3* were abundant at the 1-cell stage and gradually decreased from the 2-cell to blastocyst stage [22]. Consistent with these findings, in our present study, the high level of *CTSB*, *CTSD*, and *CTSZ* gene expression in MII oocytes suggests that the mRNA are transcripts completely derived from maternal proteins until the 8-cell stage when maternal mRNA are completely degraded. These findings reflect the transition from maternal to embryonic genome transcription of lysosomal CTSs during bovine oocyte maturation and preimplantation embryo development. Consistent with our findings, it was also verified in *in vitro*- or *in vivo*- derived bovine and mouse blastocysts that KEGG pathways enriched for the genes of *CTSA*, *CTSB*, *CTSD*, *CTSH*, and *CTSL* were upregulated in the TE [23, 24]. The TE is fated to be the cell lineage through which the blastocyst interacts directly with the mother in regards to nutrient exchange, maternal-conceptus communication, and placentation. It has been demonstrated that inhibition of CTSB, *L in vivo* at the stage of blastocyst attachment resulted in complete failure of implantation or stunted embryos and a reduced decidual reaction, suggesting that CTSB and CTSL are necessary for normal embryo development and uterine decidualization in mice [9]. Taken together, our results suggest a new mechanism of CTSs on the different function of ICM and TE with differentiated status.

In many animal species, the transformation from differentiated oocyte to totipotent embryo after fertilization, known as the oocyte-to-embryo transition, is crucial for further embryonic development. As this transition is accomplished during a short period, the embryo must stimulate vast degradation systems in order to eliminate unnecessary maternal factors and recycle them for use in the synthesis of new zygotic products. After fertilization, our results showed that CTSB and lysosomal activity was highest at one-cell stage which supported with previous report that autophagy is highly induced after fertilization [25].

Lysosomes are specialized organelles involved in macromolecular degradation processes. Accumulating evidence has demonstrated that lysosomes have many physiological functions. Mutations in many genes involved in lysosomal biogenesis have been revealed to be associated with lysosomal dysfunction [20, 26]. In recent years, the functional analysis of lysosomes in mouse preimplantation embryos revealed that the number of lysosomes increased after fertilization, and lysosomes were abundant during mouse preimplantation development until the morula stage, but their numbers decreased slightly in blastocysts [12]. In addition, 1-cell embryos injected with siRNA that targeted both LAMP1 and LAMP2 were developmentally arrested at the 2-cell stage [12]. Consistent with these findings, we found that fluorescence intensity of lysosomes was increased at one-cell stage after fertilization, and also that intensity significantly increased in the morula stage and decreased in the blastocyst stage. In addition, the fluorescence intensity of lysosomes was significantly higher in the ICM area compared to the TE area in both intact and dissected blastocysts. Considering that lysosomes typically constitute 0.5% to 5% of the cell volume [19], our findings suggest that degradation via lysosomes is highly activated in zygotes and morulae as well as in the ICM.

We found that CTSB activity was significantly increased in 1-cell stage embryos and slightly decreased in 2-cell to 8-cell stage embryos, but significantly increased in the morula stage again, and declined in the blastocyst stage. These dynamic changes were consistent with that of lysosomal activity. Similar with these results, it has been demonstrated that autophagy is highly activated after fertilization [25]. Moreover, during the morula stage, cells on the outer part of the morula become tightly bound together with the formation of desmosomes and gap junctions, a process known as compaction [27] and is the start time of differentiation. Following subsequent cleavages, a cavity forms inside the morula, and results in a hollow ball of cells known as the blastocyst [28]. Therefore, the dynamic changes of CTSB activity from morula to blastocyst probably revealed the role of CTSB on cytoplasm catabolic activity during differentiation of bovine preimplantation embryo development.

We subsequently analyzed the protein distribution of CTSB in oocytes and preimplantation embryos. We found that CTSB protein displayed a generally uniform distribution in the cytoplasm of the oocyte stages, but was detected with stronger fluorescence in the cytoplasm of morulae and blastocysts, and the fluorescence intensity was significantly higher in the cytoplasm of morulae and blastocysts than MII oocytes. Although a clear correlation of immunostaining and activity of CTSB was not observed, the increasing pattern of the fluorescence of CTSB and activity from GV/MII to morula indicates the similar profile of protein and activity. Another possible explanation could be caused by the two forms CTSB i.e active and inactive forms [29, 30]. It is necessary to detect the two forms of CTSB in the next analysis.

Recently, matured CTSB protein was detected in the 2-cell to morula stage, while the amount dramatically decreased in the blastocyst stage of mouse embryos [12]. This opposite dynamic pattern in the blastocyst stage compared to the results of our study may be attributed to the difference of animal species used. However, including our results, these data suggest the functional conversion of CTSB during bovine preimplantation development, especially in the morula stage. In addition, the fluorescence intensity exhibited a high tendency of localization in the cytoplasm of blastocysts compared to GV oocytes. Our findings are similar to that of Kim *et al.*, who found a weak signal of CTSB protein in 1- to 4-cell stage of porcine embryos, and a clustered localization pattern in morulae and blastocysts [15]. Taken together, these results highlight the important role of CTSB and lysosomes in bovine embryo development and differentiation.

Interestingly, we found a completely opposite pattern between gene expression and both protein distribution and the enzymatic activity of CTSB in the ICM and TE at the blastocyst stage.

Highly active CTSB with increased protein level showed a similar pattern of lysosomal activation in ICM compared with TE cells. This opposite pattern could be explained by the different turnover rate of CTSB by consumption of mRNA in the ICM and TE, whereby the low CTSB level in the ICM could not be caused by the down regulation of the *CTSB* gene, but rather potential high turnover of CTSB used for protein synthesis and enzymatic reaction for the potential role of differentiation. This phenomenon could be supported by the activation of lysosome, that contributes the protein turn over.

Recent research has revealed the correlation of lysosome and CTS with autophagy [5]. Future research is necessary to investigate the

detail mechanisms of CTS, lysosome and potential role of autophagy in the development and differentiation of bovine embryos.

In conclusion, we investigated the gene expression pattern of CTS in the early development of bovine embryos, and patterns of CTSB and lysosomal activities in a stage-specific and, as well as CTSB protein distribution during oocyte maturation and preimplantation development of bovine embryos.

Acknowledgement

This study was supported by a Grant-in-Aid for Scientific Research from the Japan Society for the Promotion of Science (KAKENHI, 24580439).

References

1. Dominko T, First NL. Timing of meiotic progression in bovine oocytes and its effect on early embryo development. *Mol Reprod Dev* 1997; **47**: 456–467. [Medline] [CrossRef]
2. Rizos D, Ward F, Duffy P, Boland MP, Lonergan P. Consequences of bovine oocyte maturation, fertilization or early embryo development in vitro versus in vivo: implications for blastocyst yield and blastocyst quality. *Mol Reprod Dev* 2002; **61**: 234–248. [Medline] [CrossRef]
3. Lindner GM, Wright RW Jr. Bovine embryo morphology and evaluation. *Theriogenology* 1983; **20**: 407–416. [Medline] [CrossRef]
4. Scott L, Alvero R, Leondires M, Miller B. The morphology of human pronuclear embryos is positively related to blastocyst development and implantation. *Hum Reprod* 2000; **15**: 2394–2403. [Medline] [CrossRef]
5. Tsukamoto S, Hara T, Yamamoto A, Kito S, Minami N, Kubota T, Sato K, Kokubo T. Fluorescence-based visualization of autophagic activity predicts mouse embryo viability. *Sci Rep* 2014; **4**: 4533. [Medline] [CrossRef]
6. Mohamed MM, Sloane BF. Cysteine cathepsins: multifunctional enzymes in cancer. *Nat Rev Cancer* 2006; **6**: 764–775. [Medline] [CrossRef]
7. Follo C, Ozzano M, Montalenti C, Santoro MM, Isidoro C. Knockdown of cathepsin D in zebrafish fertilized eggs determines congenital myopathy. *Biosci Rep* 2013; **33**: e00034. [Medline] [CrossRef]
8. Sol-Church K, Shipley J, Beckman DA, Mason RW. Expression of cysteine proteases in extraembryonic tissues during mouse embryogenesis. *Arch Biochem Biophys* 1999; **372**: 375–381. [Medline] [CrossRef]
9. Afonso S, Romagnano L, Babiartz B. The expression and function of cystatin C and cathepsin B and cathepsin L during mouse embryo implantation and placentation. *Development* 1997; **124**: 3415–3425. [Medline]
10. Song G, Spencer TE, Bazer FW. Cathepsins in the ovine uterus: regulation by pregnancy, progesterone, and interferon tau. *Endocrinology* 2005; **146**: 4825–4833. [Medline] [CrossRef]
11. Spencer TE, Johnson GA, Bazer FW, Burghardt RC, Palmarini M. Pregnancy recognition and conceptus implantation in domestic ruminants: roles of progesterone, interferons and endogenous retroviruses. *Reprod Fertil Dev* 2007; **19**: 65–78. [Medline] [CrossRef]
12. Tsukamoto S, Hara T, Yamamoto A, Ohta Y, Wada A, Ishida Y, Kito S, Nishikawa T, Minami N, Sato K, Kokubo T. Functional analysis of lysosomes during mouse preimplantation embryo development. *J Reprod Dev* 2013; **59**: 33–39. [Medline]
13. Seshagiri PB, Sen Roy S, Sireesha G, Rao RP. Cellular and molecular regulation of mammalian blastocyst hatching. *J Reprod Immunol* 2009; **83**: 79–84. [Medline] [CrossRef]
14. Sen Roy S, Seshagiri PB. Expression and function of cyclooxygenase-2 is necessary for hamster blastocyst hatching. *Mol Hum Reprod* 2013; **19**: 838–851. [Medline] [CrossRef]
15. Kim SH, Zhao MH, Liang S, Cui XS, Kim NH. Inhibition of cathepsin B activity reduces apoptosis by preventing cytochrome c release from mitochondria in porcine parthenotes. *J Reprod Dev* 2015; **61**: 261–268. [Medline] [CrossRef]
16. Balboula AZ, Yamanaka K, Sakatani M, Hegab AO, Zaabel SM, Takahashi M. Intracellular cathepsin B activity is inversely correlated with the quality and developmental competence of bovine preimplantation embryos. *Mol Reprod Dev* 2010; **77**: 1031–1039. [Medline] [CrossRef]
17. Balboula AZ, Yamanaka K, Sakatani M, Hegab AO, Zaabel SM, Takahashi M. Cathepsin B activity is related to the quality of bovine cumulus oocyte complexes and its inhibition can improve their developmental competence. *Mol Reprod Dev* 2010; **77**: 439–448. [Medline] [CrossRef]

18. **Balboula AZ, Yamanaka K, Sakatani M, Kawahara M, Hegab AO, Zaabel SM, Takahashi M.** Cathepsin B activity has a crucial role in the developmental competence of bovine cumulus-oocyte complexes exposed to heat shock during in vitro maturation. *Reproduction* 2013; **146**: 407–417. [Medline] [CrossRef]
19. **Matteoni R, Kreis TE.** Translocation and clustering of endosomes and lysosomes depends on microtubules. *J Cell Biol* 1987; **105**: 1253–1265. [Medline] [CrossRef]
20. **Saftig P, Klumperman J.** Lysosome biogenesis and lysosomal membrane proteins: trafficking meets function. *Nat Rev Mol Cell Biol* 2009; **10**: 623–635. [Medline] [CrossRef]
21. **Kues WA, Sudheer S, Herrmann D, Carnwath JW, Havlicek V, Besenfelder U, Lehrach H, Adjaye J, Niemann H.** Genome-wide expression profiling reveals distinct clusters of transcriptional regulation during bovine preimplantation development in vivo. *Proc Natl Acad Sci USA* 2008; **105**: 19768–19773. [Medline] [CrossRef]
22. **Xu YN, Shen XH, Lee SE, Kwon JS, Kim DJ, Heo YT, Cui XS, Kim NH.** Autophagy influences maternal mRNA degradation and apoptosis in porcine parthenotes developing in vitro. *J Reprod Dev* 2012; **58**: 576–584. [Medline] [CrossRef]
23. **Hosseini SM, Dufort I, Caballero J, Moulavi F, Ghanaei HR, Sirard MA.** Transcriptome profiling of bovine inner cell mass and trophectoderm derived from in vivo generated blastocysts. *BMC Dev Biol* 2015; **15**: 49. [Medline] [CrossRef]
24. **Ozawa M, Sakatani M, Yao J, Shanker S, Yu F, Yamashita R, Wakabayashi S, Nakai K, Dobbs KB, Sudano MJ, Farmerie WG, Hansen PJ.** Global gene expression of the inner cell mass and trophectoderm of the bovine blastocyst. *BMC Dev Biol* 2012; **12**: 33. [Medline] [CrossRef]
25. **Tsukamoto S, Kuma A, Murakami M, Kishi C, Yamamoto A, Mizushima N.** Autophagy is essential for preimplantation development of mouse embryos. *Science* 2008; **321**: 117–120. [Medline] [CrossRef]
26. **Reiser J, Adair B, Reinheckel T.** Specialized roles for cysteine cathepsins in health and disease. *J Clin Invest* 2010; **120**: 3421–3431. [Medline] [CrossRef]
27. **Tim C, Richard L.** Basic Sciences for Obstetrics and Gynaecology. Springer-Verlag Berlin and Heidelberg GmbH & Co. K; 1995; 18.
28. **Geisert RD, Malayer JR.** Implantation: blastocyst formation. In: Hafez B, Hafez Elsayed SE (eds.), *Reproduction in Farm Animals*. Wiley; 2000; 118.
29. **Bühling F, Fengler A, Brandt W, Welte T, Ansoorge S, Nägler DK.** Review: novel cysteine proteases of the papain family. *Adv Exp Med Biol* 2000; **477**: 241–254. [Medline] [CrossRef]
30. **Turk B, Turk D, Turk V.** Lysosomal cysteine proteases: more than scavengers. *Biochim Biophys Acta* 2000; **1477**: 98–111. [Medline] [CrossRef]